Publication Year	2017
Acceptance in OA	2020-07-21T12:07:08Z
Title	Spectral analysis of Ahuna Mons from Dawn mission's visible-infrared spectrometer
Authors	ZAMBON, Francesca, RAPONI, Andrea, TOSI, Federico, DE SANCTIS, MARIA CRISTINA, McFadden, L. A., CARROZZO, FILIPPO GIACOMO, LONGOBARDO, ANDREA, CIARNIELLO, Mauro, Krohn, K., Stephan, K., PALOMBA, Ernesto, Pieters, C. M., Ammannito, E., Russell, C. T., Raymond, C. A.
Publisher's version (DOI)	10.1002/2016GL071303
Handle	http://hdl.handle.net/20.500.12386/26547
Journal	GEOPHYSICAL RESEARCH LETTERS
Volume	44

AGU PUBLICATIONS

Geophysical Research Letters

RESEARCH LETTER
10.1002/2016GL071303

Key Points:
- Spectral analysis of Ahuna Mons reveals compositional variations that reflect multiple episodes of cryovolcanic extrusion on Ceres' surface
- Spectral parameter analysis of Ahuna Mons shows a gradient in the composition and abundance of carbonates
- Thermal variations observed in Ahuna Mons indicate different compactness of the surface regolith in specific locations

Correspondence to:
F. Zambon,
francesca.zambon@iaps.inaf.it

Citation:
Zambon, F., et al. (2016), Spectral analysis of Ahuna Mons from Dawn mission's visible-infrared spectrometer, *Geophys. Res. Lett.*, *43*, doi:10.1002/2016GL071303.

Received 11 OCT 2016
Accepted 14 DEC 2016
Accepted article online 15 DEC 2016

©2016. American Geophysical Union. All Rights Reserved.

Spectral analysis of Ahuna Mons from Dawn mission's visible-infrared spectrometer

F. Zambon[1], A. Raponi[1], F. Tosi[1], M. C. De Sanctis[1], L. A. McFadden[2], F. G. Carrozzo[1], A. Longobardo[1], M. Ciarniello[1], K. Krohn[3], K. Stephan[3], E. Palomba[1], C. M. Pieters[4], E. Ammannito[5], C. T. Russell[5], and C. A. Raymond[6]

[1]Istituto di Astrofisica e Planetologia Spaziali, INAF, Rome, Italy, [2]Goddard Space Flight Center, Greenbelt, Maryland, USA, [3]Institute of Planetary Research, German Aerospace Center (DLR), Berlin, Germany, [4]Department of Earth, Environmental, and Planetary Sciences, Brown University, Providence, Rhode Island, USA, [5]Earth Planetary and Space Sciences, University of California, Los Angeles, California, USA, [6]NASA Jet Propulsion Laboratory and California Institute of Technology, Pasadena, California, USA

Abstract Ahuna Mons is the highest mountain on Ceres. A unique complex in terms of size, shape, and morphology, Ahuna is bordered by flanks of the talus around its summit. Recent work by Ruesch et al. (2016) based on Dawn's Framing Camera images shed light on the possible origin of Ahuna Mons. According to Ruesch et al. (2016), Ahuna Mons is formed by a volcanic process involving the ascent of cryomagma and extrusion onto the surface followed by dome development and subsequent spreading. Here we analyzed in detail the composition of Ahuna Mons, using data acquired by the visible and infrared spectrometer aboard Dawn. The spectral analysis reveals a relatively high abundance of carbonates and a nonhomogeneous variation in carbonate composition and abundance along Ahuna's flanks, associated with a lower amount of the Ceres's ubiquitous NH_4-phyllosilicates over a large portion of the flanks. The grain size is coarser on the flanks than in the surrounding regions, suggesting the presence of fresher material, also compatible with a larger abundance of carbonates. Thermal variations are seen in Ahuna, supporting the evidence of different compactness of the surface regolith in specific locations. Results of the spectral analysis are consistent with a possible cryovolcanic origin which exposed fresher material that slid down on the flanks.

1. Introduction

Ceres, the largest object in the main asteroid belt, and second target of the NASA's Dawn mission, attracted the interest of many researchers over the last decades. Past ground-based spectroscopic observations of Ceres revealed the existence of an absorption band at ~3 μm. This feature was interpreted as due to structural OH groups and adsorbed or interlayer H_2O molecules in clay minerals, inferring that the dominant minerals on the surface of Ceres were hydrated clay minerals structurally similar to terrestrial montmorillonite [*Lebofsky*, 1978; *Lebofsky et al.*, 1981]. *Larson et al.* [1979] suggested that the surface of Ceres was compatible with mixtures of opaque materials and hydrated silicates. Other authors suggested that the 3.07 μm band could be due to ammoniated phyllosilicates, specifically ammonium-bearing saponite [*King et al.*, 1992] or hydrated smectite clays [*Feierberg et al.*, 1981]. *Rivkin et al.* [2006] associated the extra absorption near the 3 μm band to Fe-rich cronstedrite and carbonates. The presence of phyllosilicates and carbonate compounds was confirmed by observations carried out with the Keck II telescope [*Carry et al.*, 2008].

Recent data acquired by the visible and infrared (VIR) mapping spectrometer onboard Dawn shed light on the overall surface composition of Ceres. The thermally corrected average spectrum of Ceres as observed by VIR reveals the presence of several absorptions in the 2.5–4 μm region [*De Sanctis et al.*, 2015]. These spectral signatures are located at 2.7 μm, 3.1 μm, 3.3–3.4 μm, and 4 μm (ibid). The 2.7-μm band is diagnostic of hydrous minerals, the 3.1-μm band is associated with NH_4-phyllosilicates, and the 3.3–3.4-μm band, when detected along with the 4-μm band, is diagnostic of carbonates [*Milliken and Rivkin*, 2009]. The application of a linear spectral unmixing model to telescopic spectra of Ceres yielded a best fit by using, as spectral end-members, Mg-bearing carbonates such as dolomite, calcite, and brucite [*Milliken and Rivkin*, 2009]. Results of the nonlinear, spectral unmixing model based on the Hapke theory [*Hapke*, 1981, 1993] indicate that this average spectrum fits quite well with a mixture of NH_4-montmorillonite or NH_4-annite, antigorite, Mg-carbonate, and a featureless dark component [*De Sanctis et al.*, 2015]. On the other hand, spectral mixtures using brucite do not provide good fits. The first spatially resolved map of Ceres obtained on the basis of Dawn optical imagery [*Nathues et al.*, 2015] revealed an overall dark surface (albedo 0.11) [*Li et al.*, 2016]

with widespread albedo variations, 38 high-albedo spots [*Palomba et al.*, 2016], and the presence of peculiar geological features seen at the local scale (0.01–1 km). Ahuna Mons is an isolated elliptical mountain (21 × 13 km) located at 10.3°S, 316.2°E. With an average height of about 4 km (5 km on its steepest side), this is the highest mountain discovered on Ceres by the Dawn mission. Although two other mountains have been identified and named (Liberalia Mons and Yamor Mons), Ahuna Mons is a unique complex with peculiar morphological characteristics [*Ruesch et al.*, 2016]. In the following, we discuss its surface composition as inferred from high-spatial-resolution spectra acquired by VIR, which complements the detailed geologic investigation carried out previously [*Ruesch et al.*, 2016].

2. Data Analysis

From June 2015 until September 2016, the Dawn mission at Ceres was divided into three phases, each characterized by a different altitude of the spacecraft over the mean surface: Survey (spacecraft altitude 4350 km, spatial resolution ~ 1.1 km/pixel), High Altitude Mapping Orbit (HAMO) (spacecraft altitude 1450 km, pixel resolution ~ 360–400 m/pixel), and Low Altitude Mapping Orbit (LAMO) (spacecraft altitude 370 km, pixel resolution ~ 90–100 m/pixel) [*Russell and Raymond*, 2011].

To investigate the composition of Ahuna Mons, we used VIR hyperspectral images acquired in the HAMO mission phase. VIR data were calibrated following the procedure described in *Filacchione and Ammannito* [2014]. Artifact-removal procedures [*Carrozzo*, 2016] and thermal-removal procedures [*Raponi et al.*, 2015] were first applied, then the Hapke model [*Hapke*, 1981, 1993] was used to provide a proper photometric correction [*Ciarniello et al.*, 2016]. VIR data were normalized to the standard illumination condition (ph = 30°, $i = 30°$, $e = 0°$), which is also the common geometry used in laboratory measurements of spectral reflectance. Comprehensive compositional information about Ahuna Mons is gathered by using three complementary approaches: (1) analysis of selected spectral parameters, (2) application of a nonlinear spectral unmixing model based on the Hapke theory, and (3) consideration of thermal properties in this region.

For our purpose, we selected those spectral parameters showing substantial variability. Unlike the 2.7- and 3.1-μm band centers, which appear quite uniform across Ceres, the 3.4- and 4-μm signatures show a larger variability in the Ahuna Mons region than globally across Ceres. For this reason we decided to discard the 2.7- and 3.1-μm band centers. To derive the band centers of the 2.7, 3.1, 3.4, and 4-μm, we follow the approach by *Cloutis et al.* [1986]. For all of the abovementioned spectral features, we also compute the band depth following the definition by *Clark and Roush* [1984]. The depth of an absorption band is indicative of the abundance of the absorbing material and is also affected by the grain size and the presence of opaque material [*Clark*, 1999]. Spectral slopes may also be used to trace compositional variability. They are diagnostic of a terrain's maturity and also provide complementary information on the grain size (ibid). We compute spectral slopes between 0.55–0.85 μm, 1.00–1.90 μm, and 1.90–2.40 μm, respectively, using the definition of *Filacchione et al.* [2012]. The spectral parameters considered in this work are shown in Figure 1.

We apply a nonlinear spectral unmixing model based on the Hapke theory to selected regions of interest within the Ahuna Mons area, to assess the most plausible mineral phases and their respective abundances (Figure 2). The same method was used earlier by *De Sanctis et al.* [2015] and *De Sanctis et al.* [2016] in their investigation of the average surface composition of Ceres based on Dawn/VIR data and on the spectral analysis of the Occator bright spot, respectively.

Our analysis is complemented by a spatially resolved, surface temperature map of the Ahuna Mons area, retrieved from VIR data in the infrared range dominated by thermal emission (Figure 3). Such a map may point out thermal anomalies, i.e., specific area whose response to insolation differs from surrounding terrains, which in principle might reveal local inhomogeneities in regolith thickness, density, or thermal conductivity. Surface temperature is retrieved in the 4.5–5.1 μm range by using the approach described in the Appendix of *Tosi et al.* [2014]. Similar maps were used in previous works focused on Dawn data obtained at Vesta [*Tosi et al.*, 2015; *Zambon et al.*, 2015].

3. Results and Implications

Ahuna Mons consists of steep (30° to 40°) flanks of talus and a slightly (~300 m deep) topographically depressed summit unit [*Ruesch et al.*, 2016]. The summit unit thus represents a brittle dome carapace, formed

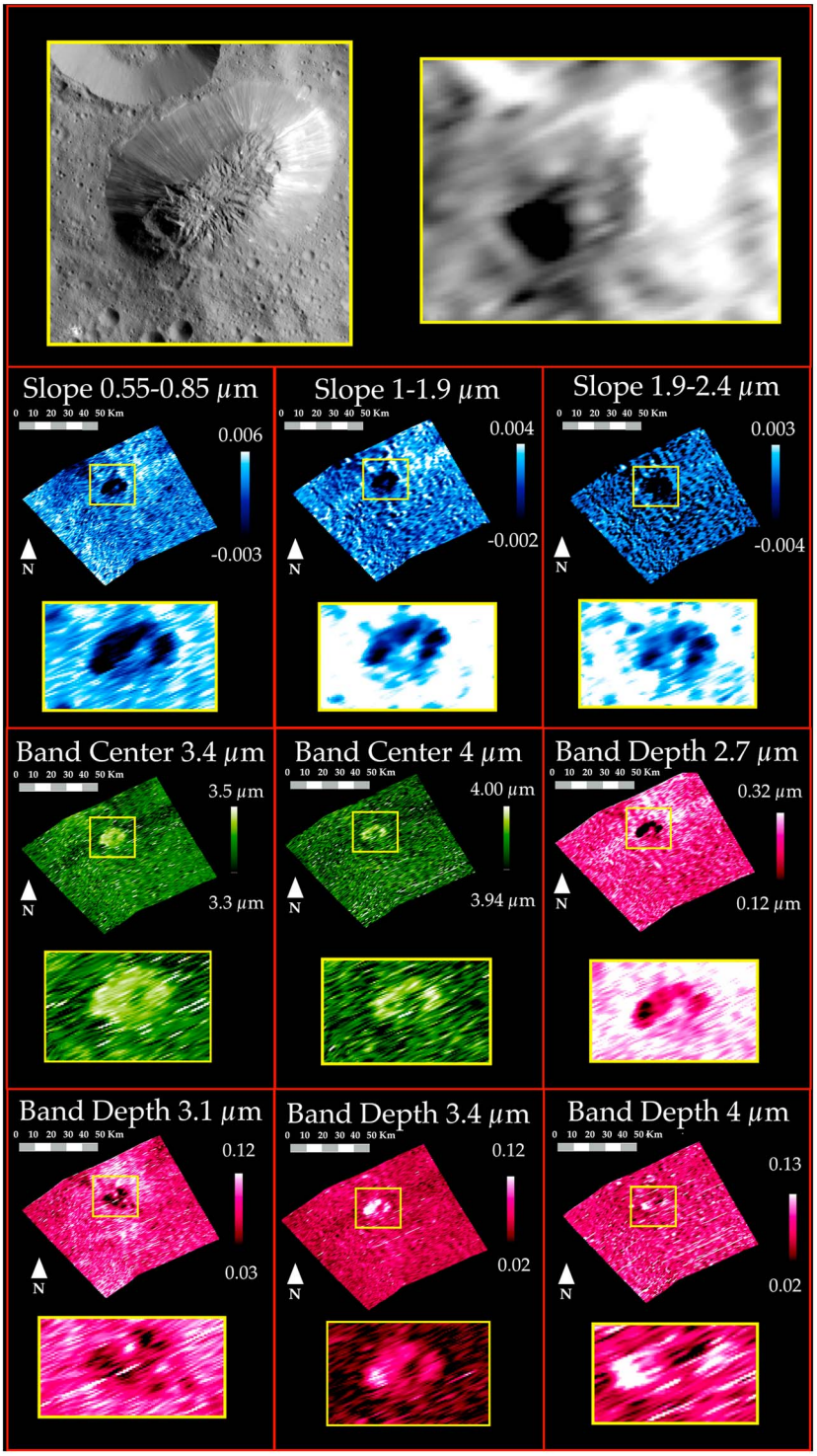

Figure 1. Equirectangular projection of the Ahuna Mons region, as observed by Dawn/Framing Camera (FC) in its clear filter in (top left) HAMO and by (top right) Dawn/VIR at 1.2 μm in LAMO. Relevant spectral parameters used to map the surface composition of Ahuna Mons include spectral slopes mapped in blue, band centers (at 3.4 and 4 μm) in green, and band depths (at 2.7, 3.1, 3.4, and 4 μm) in magenta. North is up.

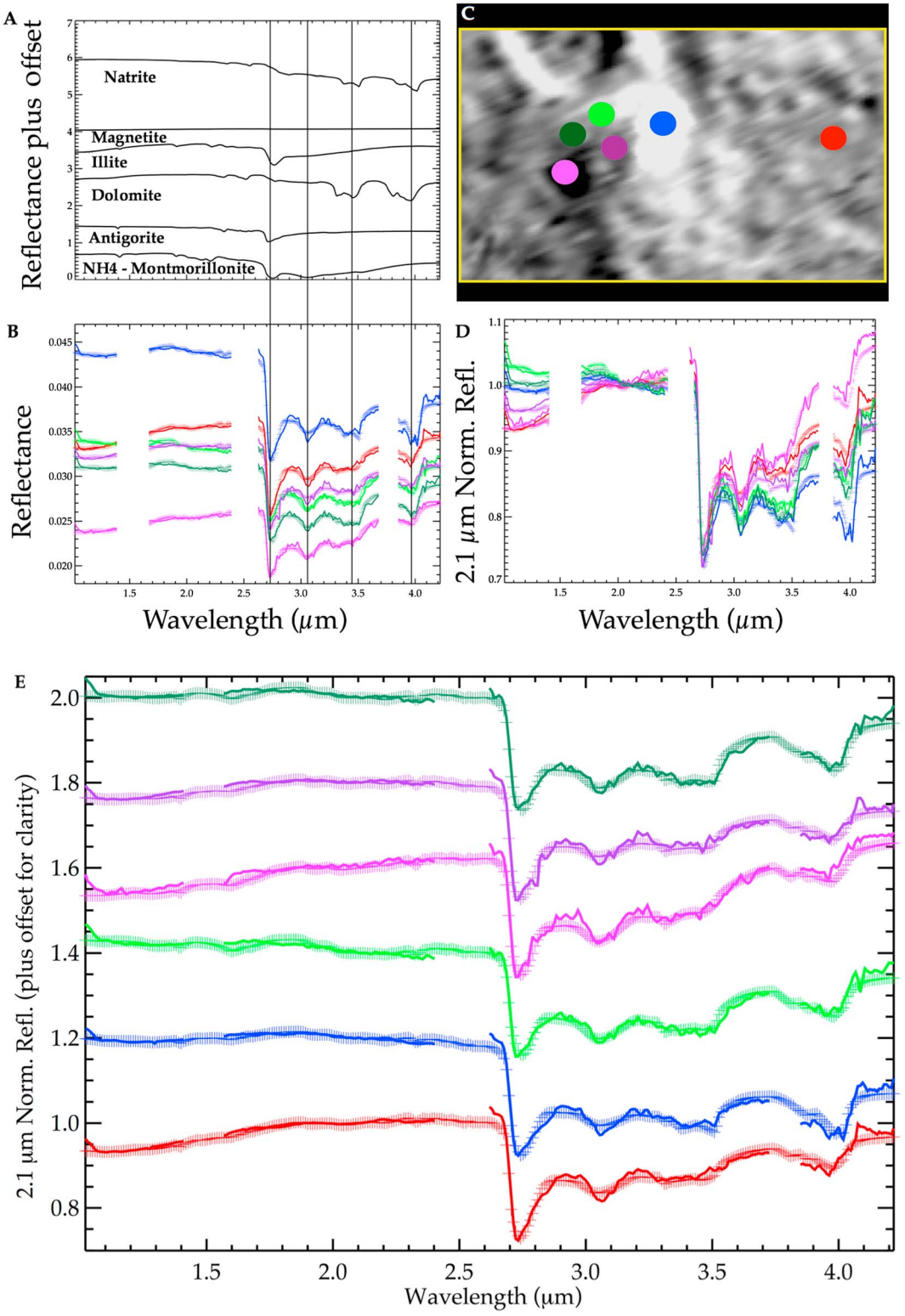

Figure 2. (a) Spectral end-member modeling the surface composition of Ahuna Mons. (b) Results of the nonlinear spectral unmixing model applied to selected regions of interest (ROIs) within the Ahuna Mons area. Different colors correspond to regions as follows: red: surrounding terrain, blue: eastern flanks, light green: northern flank, dark green: north-western flank, magenta: western flank, purple: summit. For each ROI, the solid line represents the average VIR spectrum, while the plus-sign line is the modeled spectrum. (c) Locations of ROIs. (d) Same spectra of Figure 2b normalized at 2.1 μm. (e) Same spectra of Figure 2b plus offset (+0.2) applied for clarity.

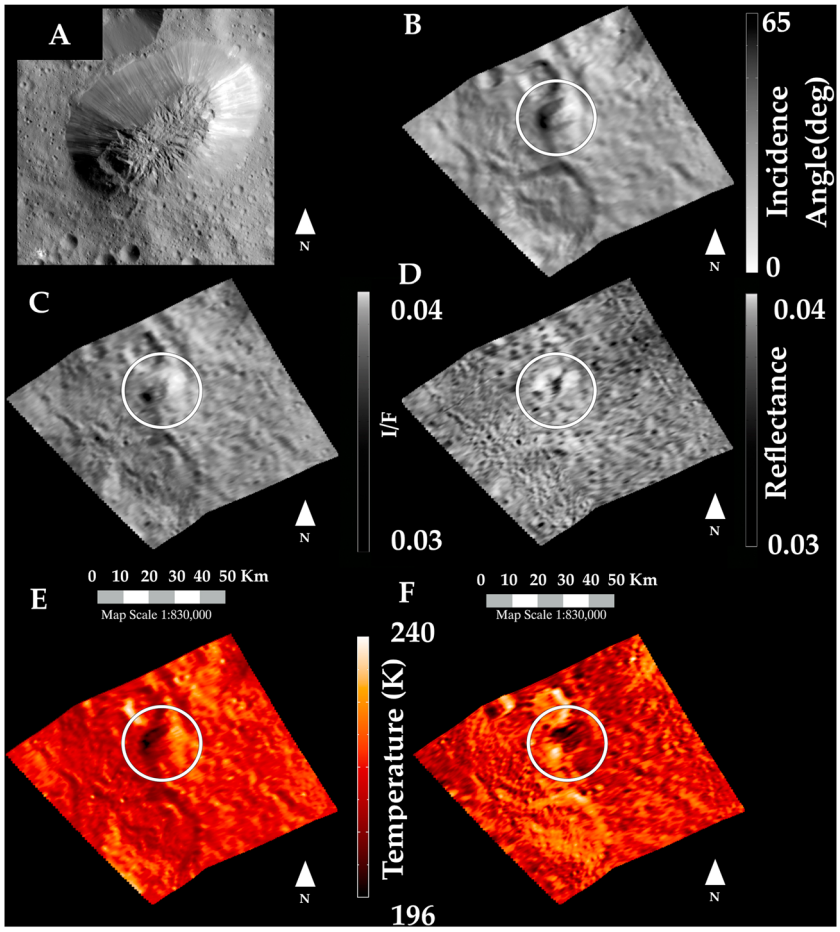

Figure 3. (a) Ahuna Mons revealed by FC (credits: NASA/Jet Propulsion Laboratory-California Institute of Technology/University of California Los Angeles/Max Planck Institute for Solar System Research/German Aerospace Center/IDA Institute for Defense Analyses) acquired in the clear filter during LAMO at a spatial resolution of 35.5 m/pixel and represented in equirectangular projection (center lat = 10.48°S, center lon = 316.2°E). (b) The solar incidence angle of radiation in the VIR image as measured for each pixel with respect to the normal to the surface element based on a detailed shape model of Ceres [*Preusker et al.*, 2016]. This information inevitably follows the trend of the topography in such a way that the materials illuminated at large incidence angles (dark tones) are generally cooler than materials illuminated at small incidence angles (bright tones). (c and d) VIR data of the same area represented in Figure 3a at 1.2 μm wavelength (scan sequence: 493234611) acquired in HAMO (360 m/pixel) at a heliocentric distance of 2.953 AU, also in equirectangular projection, before and after application of a Hapke photometric correction, respectively. (e) Surface temperature map as derived from VIR spectra in the range of 4.5–5.1 μm. (f) Surface temperature after rough correction for the local topography. A horizontal scale bar accounts for the size of the features observed in the scene. For a body like Ceres, which has an overall low thermal inertia, the main parameter driving the surface temperature is the solar incidence angle. Assuming that the surface of Ceres ideally behaves as a blackbody, dividing the surface temperature for the fourth root of the cosine of the solar incidence angle (Figure 3f) is a quick way to highlight possible thermal anomalies occurring at the local scale.

by cooling of the outermost region of a ductile core. The fracturing of the carapace leads to its partial disintegration and production of boulders and smaller debris (ibid).

For our analysis, we selected six regions of interest (ROIs) inside and outside Ahuna Mons as displayed in Figure 2c: the light and dark green areas (northern flank), the blue area (eastern flank), the magenta area (western flank), the purple area (summit unit), and the red area (surrounding).

A close inspection of the Ahuna Mons region reveals spectral differences between the flanks, the summit, and the surroundings. We observe spectral variations at different portions of the summit and flanks in the following analysis. Occurrence of both high-albedo (bright) and low-albedo (dark) materials has also been observed. After applying photometric correction, the 1.2-μm reflectance image (Figure 3d) shows that the flanks of the mountain are characterized by bright material, while the summit is inherently darker than the

Table 1. Results Obtained by Our Spectral Unmixing Model[a]

	Regions											
End-Member	Red	SD	Blue	SD	Light Green	SD	Magenta	SD	Purple	SD	Dark Green	SD
NH4-mont (%)	4.9	1.1	3.9	0.4	5.2	0.3	4.9	0.4	*3.5*	*0.8*	**5.7**	**0.4**
Dark phase (%)	*80.3*	*2.9*	82.2	1.9	87.0	1.0	**88.4**	**1.5**	84.1	3.2	81.8	4.0
Antigorite (%)	**7.9**	**1.1**	5.9	1.0	*4.1*	*0.5*	4.7	1.0	6.6	1.5	5.3	1.7
Illite (%)	**2.3**	**0.7**	**2.3**	**0.5**	*0.0*	*0.0*	0.3	0.2	**2.3**	**1.1**	1.4	1.3
Dolomite (%)	**2.4**	**0.5**	*1.1*	*0.2*	1.9	0.3	1.6	0.1	1.8	0.5	2.1	0.6
Natrite (%)	2.2	0.6	*1.1*	*0.4*	2.3	0.3	1.2	0.1	1.9	0.4	**4.4**	**0.4**
Grain size (μm)	*56.9*	*7.1*	76.0	11.4	**121.8**	**5.3**	97.6	7.8	72.0	12.1	118.4	38.6
χ^2	0.789		0.515		1.048		1.225		0.636		1.045	
Carbonate tot. (%)	4.6	0.6	5.9	0.4	4.1	0.3	*2.8*	*0.1*	3.7	0.5	**6.5**	**0.4**

[a]We report only the values of the most relevant end-members. Numbers in bold indicate the highest values found for each end-member, while numbers in italic indicate the lowest values.

flanks. Maps of the relevant spectral parameters (Figure 1) show the following clear trends within this region. All three measured spectral slopes are smaller in Ahuna Mons flanks with respect to the surroundings (Figure 1), which could be consistent with either a coarser regolith, as inferred from spectral modeling, or a younger age and/or a larger amount of carbonates [*Clark*, 1999].

The center of the 2.7-μm and 3.1-μm bands is quite homogeneous throughout the considered region; thus, no compositional variation in the mineralogical phases of OH-rich material and ammoniated phyllosilicates is observed, whereas band depths of the Ahuna Mons flanks are lower than the summit regions (Figure 1). In particular, the 3.1-μm band depth is uniformly low along the flanks, except for the northern flank which has the same band depth as the surrounding background material, while the 2.7-μm band depth is generally shallower in the Ahuna flanks (Figure 1) except in the southern flanks region that has the same spectral characteristics as those of surrounding terrains. Assuming that the grain size is quite uniform in the overall Ahuna region, the decrease in the 2.7- and 3.1-μm band depth may be attributed to a lower abundance of OH-bearing phases and of NH_4-phyllosilicates, respectively (Figure 1 and Table 1).

As opposed to the 2.7- and 3.1-μm band centers, the 3.4-μm and the 4-μm band centers are shifted toward longer wavelengths in the spectra of the flanks of Ahuna Mons, compared to the surroundings and the summit. This indicates a variability within Ahuna Mons complex, suggesting a gradient in the composition of carbonates.

Application of the Hapke nonlinear spectral unmixing model to the selected ROIs within and outside Ahuna Mons confirms the results we obtained by using the spectral parameters analysis (Figure 2). In Table 1, we report the results obtained with our unmixing model. The model clearly indicates that this entire area is dominated by a dark featureless component (abundance >80%), like most of Ceres surface [*De Sanctis et al.*, 2015]. As indicated by the spectral parameters, the surrounding area (red spectra in Figure 2) has a composition clearly different from Ahuna Mons flanks.

The northern flank appears rich in ammoniated species (light and dark green points in Figure 2c) compared to the other regions, while the other flanks show a lower or a similar amount of these phases with respect to the surroundings (red). An area outside Ahuna (red) displays a consistent amount of NH_4-phyllosilicates and a larger amount of OH-rich material (named antigorite and illite in Table 1) and Mg-Ca carbonates (named dolomite in Table 1). The northern flank of Ahuna (dark green points in Figure 2c) is characterized by the highest amount of carbonates (Mg-Ca carbonates + Na-carbonates) and differs up to 3.7% with respect to the lower value observed in the western side. The Na-carbonate (named natrite in Table 1) amount in Ahuna is often higher than that of the Mg-Ca carbonates; in particular, the northern flank (light and dark green) is the area richest in Na-carbonates observed in the Ahuna region.

Ca-Mg carbonate forms in aqueous environments as evaporation from sedimentary processes [*Deer et al.*, 1992; *Deelman*, 1999]. On Earth, dolomites are usually found in mountains formed after the Permian period where oceans existed. Na-carbonate, or natrite, formed when the composition of the magma reservoir

changed and excess Na bonded with carbonate ions [*Warren*, 2016]. On Ceres, this hypothesis seems unlikely. Alternatively, natrite is found in terrestrial alkaline hydrothermal and evaporitic environments. In our solar system, it is also detected in Enceladus' plumes, along with $NaHCO_3$ and NaCl [*Postberg et al.*, 2011]. Na-carbonates are endogenous on Ceres and are representative of subsurface layers. Results from our spectral fits do not suggest the presence of $NaHCO_3$ and NaCl. *De Sanctis et al.* [2016] argued that the presence of Na-carbonates in Occator's main bright spot (Cerealia Facula) may be due to a Solvay process, i.e., the industrial process usually adopted to produce Na_2CO_3. In Ahuna Mons, Na-carbonates have been exposed after multiple cryomagmatic episodes.

Ruesch et al. [2016] proposed that Ahuna Mons was formed by a volcanic process involving the ascent of cryomagma and extrusion onto the surface followed by dome development. The mons and tholus upon which it sits might have shared a common reservoir at depth. Their different morphologies might be related to a change in the rheological properties (e.g., chemistry and temperature) of the reservoir with time or during ascent.

A thermal survey of Ahuna Mons and its surroundings reveals shades that are generally the result of instantaneous solar illumination combined with the local topography at the time of the VIR observation (Figure 3). Correction of surface temperature (Figure 3f) by the solar incidence angle highlights that the northern flank and (to a lesser extent) the summit of Ahuna could be inherently cooler than the surrounding regions observed at the same local time. Because surface composition is quite homogeneous within Ahuna Mons, this evidence could be related to a different compactness of the surface regolith in these areas. Furthermore, the derived values of grain size indicate that, generally, the flanks have a coarser grain size than the surroundings, reaching the maximum value in the eastern side. Following this hypothesis, the material on the flanks represents fresher material that slid nonuniformly down the flanks.

4. Conclusions

Spectroscopic analysis of the reflectance spectra of the Ahuna Mons region using Dawn/VIR data indicates that this geologic unit is spectrally distinct from the surrounding regions with respect to a series of diagnostic spectral indicators, namely, spectral slopes and absorption band centers and band depths at 2.7, 3.1, 3.4, and 4 μm, which are attributable to hydrous minerals, NH_4-phyllosilicates, and carbonates, respectively. Although the overall composition is not too dissimilar to what is found elsewhere on Ceres, at the local scale Ahuna Mons emerges to have a lower abundance of hydrous mineral phases and a greater abundance of Na-carbonates than the surrounding areas observed at the same spatial resolution. We observe a nonuniform composition in the Ahuna Mons flanks. In particular, the northern flanks show a larger carbonates amount than the other regions. Na-carbonates have been identified as the major constituent of the bright areas in Occator crater [*De Sanctis et al.*, 2016]. As found in Occator, spectroscopic investigation corroborated by a robust spectral unmixing model confirms that Ahuna Mons is definitely a peculiar structure with respect to composition. Its flanks are brighter and show coarser grain size than the surrounding regions, suggesting a younger age. This is confirmed by a generally greater abundance of carbonates in Ahuna compared to the surroundings, particularly in its north-west side (light and dark green regions of interest in Figure 2c). The presence of Na-carbonates has been interpreted as evidence of recent hydrothermal activity [*De Sanctis et al.*, 2016] and is consistent with a cryovolcanic origin of Ahuna Mons, which would locally raise a portion of terrain by exposing fresh subsurface material richer in carbonates.

Acknowledgments
VIR is funded by the Italian Space Agency (ASI) and was developed under the leadership of INAF-Istituto di Astrofisica e Planetologia Spaziale, Rome, Italy. The instrument was built by Selex-Galileo, Florence, Italy. The authors acknowledge the support of the Dawn Science, Instrument, and Operations Teams. This work was supported by ASI and NASA. The data used for this analysis are available at http://sbn.psi.edu/pds/resource/dwncvir.html.

References

Carrozzo, F. G. (2016), Artifacts reduction in VIR/DAWN data, in 41st COSPAR scientific assembly, abstracts from the meeting that was to be held 30 July - 7 August at the Istanbul Congress Center (ICC), Turkey, but was cancelled. See <A href=. [Available at http://cospar2016.tubitak.gov.tr/en/">http://cospar2016.tubitak.gov.tr/en/</A>, Abstract B0.4-42-16., COSPAR Meeting, vol. 41.]

Carry, B., C. Dumas, M. Fulchignoni, W. J. Merline, J. Berthier, D. Hestroffer, T. Fusco, and P. Tamblyn (2008), Near-infrared mapping and physical properties of the dwarf-planet Ceres, *Astron. Astrophys.*, *478*(1), 235–244, doi:10.1051/00046361:20078,166.

Ciarniello, M., et al. (2016), Spectrophotometric properties of dwarf planet Ceres from VIR onboard Dawn mission, *Astron. Astrophys.*, doi:10.1051/0004-6361/201629490.

Clark, R. N. (1999), *Remote Sensing for the Earth Sciences—Manual of Remote Sensing*, vol. 3, John Wiley, New York.

Clark, R. N., and T. L. Roush (1984), Reflectance spectroscopy: Quantitative analysis techniques for remote sensing applications, *J. Geophys. Res.*, *89*, 6329–6340, doi:10.1029/JB089iB07p06,329.

Cloutis, E. A., M. J. Gaffey, T. L. Jackowski, and K. L. Reed (1986), Calibrations of phase abundance, composition, and particle size distribution for olivine-orthopyroxene mixtures from reflectance spectra, *J. Geophys. Res.*, *91*, 641–653, doi:10.1029/JB091iB11p11,641.

De Sanctis, M. C., et al. (2015), Ammoniated phyllosilicates with a likely outer solar system origin on (1) Ceres, *Nature*, *528*(7581), 241–244, doi:10.1038/nature16,172.
De Sanctis, M. C., et al. (2016), Bright carbonate deposits as evidence of aqueous alteration on Ceres, *Nature*, doi:10.1038/nature18,290.
Deelman, J. C. (1999), Low-temperature nucleation of magnesite and dolomite, *N. J. Miner. Monatshefte*, *7*, 289–301.
Deer, W. A., R. A. Howie, and J. Zussman (1992), *An Introduction to the Rock-Forming Minerals*, Longman Scientific & Technical, John Wiley, New York.
Feierberg, M. A., L. A. Lebofsky, and H. P. Larson (1981), Spectroscopic evidence for aqueous alteration products on the surfaces of low-albedo asteroids, *Geochim. Cosmochim. Acta*, *45*, 971–981, doi:10.1016/0016-7037(81)90,121-6.
Filacchione, G., and E. Ammannito (2014), Dawn VIR calibration document. Version 2.4. [Available at http://sbn.psi.edu/archive/dawn/vir/DWNVVIR_I1B/DOCUMENT/VIR_CALIBRATION/VIR_CALIBRATION_V2_4.PDF.]
Filacchione, G., et al. (2012), Saturn's icy satellites and rings investigated by Cassini–VIMS: III—Radial compositional variability, *Icarus*, *320*, 1064–1096, doi:10.1016/j.icarus.2012.06.040.
Hapke, B. (1981), Bidirectional reflectance spectroscopy. I - Theory, *J. Geophys. Res.*, *86*, 3039–3054, doi:10.1029/JB086iB04p03,039.
Hapke, B. (1993), *Theory of Reflectance and Emittance Spectroscopy*, Cambridge Univ. Press, Cambridge.
King, T. V. V., R. N. Clark, W. M. Calvin, D. M. Sherman, and R. H. Brown (1992), Evidence for ammonium-bearing minerals on Ceres, *Science*, *255*, 1551–1553, doi:10.1126/science.255.5051.1551.
Larson, H. P., M. A. Feierberg, U. Fink, and H. A. Smith (1979), Remote spectroscopic identification of carbonaceous chondrite mineralogies Applications to Ceres and Pallas, *Icarus*, *39*, 257–271, doi:10.1016/0019-1035(79)90,168-4.
Lebofsky, L. A. (1978), Asteroid 1 Ceres—Evidence for water of hydration, *Mon. Not. R. Astron. Soc.*, *182*, 17P–21P, doi:10.1093/mnras/182.1.17P.
Lebofsky, L. A., M. A. Feierberg, A. Tokunaga, H. P. Larson, and J. Johnson (1981), The 1.7- to 4.2-micron spectrum of asteroid 1 Ceres—Evidence for structural water in clay minerals, *Icarus*, *48*, 453–459, doi:10.1016/0019-1035(81)90,055-5.
Li, J.-Y., et al. (2016), Surface albedo and spectral variability of Ceres, *Astrophys. J.*, *817*, L22, doi:10.3847/2041-8205/817/2/L22.
Milliken, R. E., and A. S. Rivkin (2009), Brucite and carbonate assemblages from altered olivine-rich materials on Ceres, *Nat. Geosci.*, *2*(4), 258–261, doi:10.1038/ngeo478.
Nathues, A., et al. (2015), Sublimation in bright spots on (1) Ceres, *Nature*, *528*, 237–240, doi:10.1038/nature15754.
Palomba, E., et al. (2016), Compositional characteristics of Ceres bright spots, in lunar and planetary science conference, *Lunar Planet. Sci. Conf.*, *47*, 2198.
Postberg, F., J. Schmidt, J. Hillier, S. Kempf, and R. Srama (2011), A salt-water reservoir a the source of a compositionally stratified plume on Enceladus, *Nature*, *474*, 620–622, doi:10.1038/nature10175.
Preusker, F., F. Scholten, K.-D. Matz, S. Elgner, R. Jaumann, T. Roatsch, S. P. Joy, C. A. Polanskey, C. A. Raymond, and C. T. Russell (2016), Dawn at Ceres shape model and rotational state, in lunar and planetary science conference, Lunar Planet. Sci. Conf., vol. 47, p. 1954.
Raponi, A., et al. (2015), Ceres spectral modelling with VIR data onboard Dawn: Method and first results, European Plane- tary Science Congress 2015, held 27 September - 2 October, 2015 in Nantes, France, 10, EPSC2015–537.
Rivkin, A. S., E. L. Volquardsen, and R. N. Clark (2006), The surface composition of Ceres: Discovery of carbonates and iron-rich clays, *Icarus*, *185*(2), 563–567, doi:10.1016/j.icarus.2006.08.022.
Ruesch, O., et al. (2016), Cryovolcanic on Ceres, *Science*, *353*(6303), doi:10.1126/science.aaf4286.
Russell, C. T., and C. A. Raymond (2011), The Dawn mission to Vesta and Ceres, *Space Sci. Rev.*, *163*, 3–23, doi:10.1007/s11,214-011-9836-2.
Tosi, F., et al. (2014), Thermal measurements of dark and bright surface features on Vesta as derived from Dawn/VIR, *Icarus*, *240*, 36–57, doi:10.1016/j.icarus.2014.03.017.
Tosi, F., et al. (2015), Mineralogical analysis of the Oppia quadrangle of asteroid (4) Vesta: Evidence for occurrence of moderate-reflectance hydrated minerals, *Icarus*, *259*, 129–149, doi:10.1016/j.icarus.2015.05.018.
Warren, J. K. (2016), *Evaporites*, Springer, Berlin.
Zambon, F., et al. (2015), Spectral analysis of the Quadrangles Av-13 and Av-14 on Vesta, *Icarus*, *259*, 181–193, doi:10.1016/j.icarus.2015.05.015.